EFDA–JET–CP(10)08/29

I. Nunes, P.J. Lomas, D.C. McDonald, G. Saibene, R. Sartori, I. Voitsekhovitch, M. Beurskens, G. Arnoux, A. Boboc, T. Eich, C. Giroud, S Heureux, E de la Luna, G. Maddison, A.C.C. Sips, H. Thomsen, T.W. Versloot and JET EFDA contributors

Confinement and Edge Studies Towards Low ρ* and ν* at JET

Confinement and Edge Studies Towards Low ρ* and ν* at JET

I. Nunes[1,2], P.J. Lomas[3], D.C. McDonald[3], G. Saibene[4], R. Sartori[4], I. Voitsekhovitch[3], M. Beurskens[3], G. Arnoux[3], A. Boboc[3], T. Eich[5], C. Giroud,[3] S Heureux[3], E de la Luna[1,6], G. Maddison[3], A.C.C. Sips[1,7], H. Thomsen[5], T.W. Versloot[8] and JET EFDA contributors*

JET-EFDA, Culham Science Centre, OX14 3DB, Abingdon, UK

[1]EFDA-CSU, Culham Science Centre, OX14 3DB, Abingdon, OXON, UK
[2]Associação EURATOM-IST, Instituto de Plasmas e Fusão Nuclear – L.A., IST, Lisboa, Portugal
[3]EURATOM-CCFE Fusion Association, Culham Science Centre, OX14 3DB, Abingdon, OXON, UK
[4]Fusion for Energy, Barcelona, Spain
[5]Max-Planck-Institut fuer Plasmaphysik, EURATOM-Assoziation, Germany
[6]Laboratorio Nacional de Fusion, Associacion EURATOM-CIEMAT, Madrid, Spain
[7]European Commission, Brussels, Belgium
[8]FOM Institute Rijnhuizen, Association EURATOM-FOM, Nieuwegein, the Netherlands
[9]Association EURATOM-VR, Department of Physics, SCI, KTH, SE-10691 Stockholm, Sweden
** See annex of F. Romanelli et al, "Overview of JET Results", (23rd IAEA Fusion Energy Conference, Daejon, Republic of Korea (2010)).*

Preprint of Paper to be submitted for publication in Proceedings of the 23rd IAEA Fusion Energy Conference, Daejon, Republic of Korea (10th October 2010 - 16th October 2010)

ABSTRACT

The size and capability of JET to reach high plasma current and field enables a study of the plasma behaviour at ion Larmor radius and collisionality values approaching those of ITER. In this paper such study is presented. The achievement of stationary type I ELMy H-modes at high current proved to be quite challenging. As the plasma current was increased, it became more difficult to achieve stationary conditions. Nevertheless, it was possible to achieve stable operation at high plasma current (up to 4.5MA) and low q_{95} (2.65-3) at JET. One of the main reasons to revisit the high plasma current experiments done in 1997 is the higher power available and the improvement of the pedestal diagnostics. Indeed, compared with previous results, higher stored energy was achieved but confinement was still degraded. The causes of this confinement degradation are discussed in the paper.

1. INTRODUCTION

In present experiments, a substantial effort has been dedicated to the study of plasma confinement and to the understanding of how to extrapolate present plasma conditions to ITER, in order to predict ITER fusion performance. A robust method to obtain and scale present results to ITER is through dimensionless parameters [1-2]. Because of its size and its capability to go to high plasma current JET is capable of achieving ν^* and ρ^* values close to those of ITER.

The first objective of ITER is to achieve $Q = 10$ in an inductive scenario at 15MA with $q_{95} = 3$. The prediction that $Q = 10$ is achievable for the ITER size, and the selected plasma current and field is largely based on the confinement scaling mentioned above, mainly derived from ELMy H-modes. Although the ITER divertor is not built to sustain repetitively the large ELMs associated to this regime, it is still necessary to understand the ELMy H-mode regime and its underlying physics. In particular, areas where large uncertainties remain are the scaling of the additional power necessary to access the H-mode regime, the power required to maintain H-mode and energy confinement enhancement factor ($H_{98(y,2)}$ [3]) of 1. The extension of the experimental database for the scaling of energy confinement to low ν^* and ρ^* and the study of the interplay of core and H-mode pedestal can contribute to this goal. Finally since present-day confinement experiments are mostly carried out with uncontrolled ELMs, the study of how ELM size impacts on pedestal properties and their effect on plasma facing components is also relevant for the extrapolation to ITER.

This paper reports on new experiments performed at JET and includes plasma currents from 2.2MA up to 4.5MA (figure 1) with β_N varying from 1.9 to 1.4 at $q_{95} \sim 2.65$ and a few discharges at $q_{95} = 3$. Although it would have been desirable to keep β_N constant for decreasing ρ^*, this was not possible for plasma currents above ~3.5MA due to the lack of additional power. It was possible to vary ρ^* by a factor of ~1.7 (3×10-3 to 5×10-3) and ν^* by a factor of ~2 (1×10^{-2} to $\sim5\times10^{-3}$). The operational space for these experiments in dimensionless parameters ν^* and ρ^* is shown in figure 2 with ITER values included for reference. The ITER values used here to calculate ρ^* and ν^* are $T_{e,vol\ avg} = 8.1$keV and $\langle n_e \rangle = 14\times10^{19}\ m^{-3}$. Within the data set, a 3 point ρ^* scan at $q_{95} = 3$ was

performed for two values of β_N (1.5 and 1.8) for I_p = 2.2, 3 and 3.5MA. The additional heating for these discharges is primarily Neutral Beam Injection (NBI) with an additional 2-4MW of Ion-Cyclotron Resonance Heating (ICRH) up to a total additional power of 27MW.

Two plasma shapes were used in these experiments differing only in the position of the strike points in the divertor and the resulting density control due to pumping efficiency. Plasma energy content and confinement were independent of the changes of plasma shapes, at all plasma currents. The experiment included both unfuelled and gas fuelled discharges. For unfuelled discharges with plasma currents above ~3.5MA it has proven difficult to maintain stationary H-mode. This behaviour was previously observed at JET [4-5], where H-modes could be accessed at low power with nonstationary conditions and $H_{98(y,2)}$<1 (averaged in time). These pulses show cyclic phases of type I ELMs with good confinement ($H_{98(y,2)}$~1) followed by phases of type III ELMs with low confinement ($H_{98(y,2)}$~0.8). In a few cases the H-mode reverted to L-mode and stayed in L-mode despite applying input power above the (scaling) threshold.

2. DATA CONSISTENCY

The data consistency for a discharge at 4.5MA during the ELMy H-mode phase was checked using TRANSP calculations with profiles for density and temperature measured by the High Resolution Thomson Scattering diagnostic (HRTS) and Electron Cyclotron Emission (ECE). In figure 3 the measured neutron rate and the total magnetic stored energy for Pulse No: 79698 are compared with those calculated by TRANSP. Both diamagnetic stored energy and DD neutron rate calculations are in line with measured values within the code and measurement uncertainties. Also shown is the neutron rate due to thermal and NBI reactions and its contribution to the total neutron rate calculated by TRANSP. In this pulse the thermal yield reaches about 58% of the total yield. The ion and electron profiles for the high current discharge are shown in figure 4. T_e and T_i are similar as expected for a high density regime (n_{e0} ~9×10^{19} m^{-3} for this example). Comparing these results with TRANSP calculations for lower plasma current pulses also show that as plasma current is increased the power deposition profiles become more off-axis as the density increases with plasma current.

3. CONFINEMENT OF HIGH CURRENT DISCHARGES

For the following analysis, only stationary discharges (steady state duration ≥ $3\tau_E$) are selected. For discharges showing variations on the plasma stored energy, density and temperature, the data is taken averaging over only the type I ELM phases. Discharges with a transition to L-mode are discarded. The highest stored energy achieved at 4.5MA steady state is ~11.5MJ for an input power of ~26.5MW with an average Greenwald fraction of ~55%. At plasma currents above 3.5MA the thermal stored energy achieved is lower than predicted.

These results are shown in figure 5(a) where the calculated thermal stored energy is compared with the stored energy predicted by the $IPB_{98(y,2)}$ scaling law. Similar behaviour was already observed in previous high current experiments in preparation for the DT1 campaign in 1997. Lack of power

was identified as the possible cause for the reduced confinement. Figure 5(b) shows a summary of the results of the experiments reported in [4]. For the recent experiments, the difference between the measured and predicted stored energy can be as large as ~18% at $I_p \sim 4.5$MA. This variation with plasma current is clearly seen in figure 6 where $H_{98(y,2)}$ is plotted as function of plasma current. $H_{98(y,2)}$ ranges from ~1.13 to ~0.87 for increasing I_p.

To extract the dependence of confinement on ρ, a scan on plasma current (2.2MA to 3.5MA) for two values of β_N (1.5 and 1.8) with $\nu^*_{vol.avg.} \sim 5\times10^{-3}$ and 7×10^{-3} respectively (gas fuelling was used to match ν^*) and $q_{95} = 3$. The normalised confinement follows the $\rho^{*-2.7}\nu^{*-0.35}$ dependence as found in [6] consistent with a gyro-Bohm like transport. The pulses from the high current data set are compared with the estimated normalised confinement time in figure 7. Normalised confinement at the lowest ρ^* (highest I_p) is seen to be systematically below the trend of the ρ^* scans. This may be due to a weaker dependence of confinement on ρ^* at low values, or changes in other parameters correlated with low ρ^*. In line with previous studies [7], heating deposition profiles become more off-axis for lower ρ^* (higher I_p), which has been predicted to reduce confinement through reduced core temperature [8]. However, temperature gradient length is approximately constant for all discharges, suggesting that this is not the cause. Compared to the higher ρ^* (lower I_p), the lower ρ^* (higher I_p) discharges have higher gas fuelling and a closer proximity to the L-H threshold, both of which have been associated with reduced confinement [9]. This is discussed further in the following sections.

4. EFFECT OF ADDITIONAL POWER AND GAS FUELLING

A critical issue for ITER is the access to H-mode with good confinement, $H_{98(y,2)} = 1$. At JET, good H-mode confinement in low triangularity plasmas is normally achieved for $P_{IN} > 1.7$ to $2P_{L-H}$ [5]. The power above the predicted P_{L-H} [10] is shown in figure 8 as a function of plasma current for these experiments. With the power available the maximum P_{LOSS}/P_{L-H} is 1.7 at 4.5MA. Stationary operation with $H_{98(y,2)} = 1$ was achieved at $I_p = 3.8$MA (with gas fuelling) with $P_{LOSS}/P_{L-H} \sim 2$-2.4, but a reduction of $H_{98(y,2)}$ was observed at $I_p > 3.8$MA for $P_{LOSS}/P_{L-H} \sim 1.8$. In order to study futher the role of input power for achieving stationary H-modes with $H_{98(y,2)} \sim 1$ at high current, a three point unfuelled plasma current scan (with Ip from 2.5MA to 3.5MA) was performed, keeping $P_{IN} \sim 2P_{L-H}$ for each plasma current. The results show that although P_{LOSS}/P_{L-H} is similar for all plasma currents, as the plasma current increases, phases of high and low confinement occur and transitions back to L-mode are observed (see for example figure 9, red traces). Due to the nonstationary character of these discharges and the increasing risk of a large disruption due to an ELM, this scan was not done at higher plasma currents. As said before, stationary discharges at high Ip were achieved by adding gas fuelling and this is discussed further in sections 5 and 6.

Figure 9 shows the evolution of the edge pedestal temperature excursions during ELMs for two discharges at 3.5MA differing only on the level of gas fuelling. At fixed P_{LOSS}/P_{L-H}, the addition of gas fuelling results in a sustained H-mode with constant average pedestal pressure (blue trace), in contrast to the case in red, where the pedestal pressure and plasma stored energy are not constant.

Based on these empirical results, gas fuelling was included in all discharges and scaled up with I_p to maintain fixed the Greenwald fraction. However, for increasing plasma current, a further increase of gas fuelling was necessary to achieve steady state conditions. This additional fuelling did not significantly change the average plasma density (constant Greenwald fraction) but resulted in higher pedestal Greenwald fraction.

5. TYPE I ENERGY LOSSES

ELMs are accompanied by a sudden burst of particles and energy from the confined plasma to the Plasma Facing Components (PFCs). The absolute size of ELMs increases with plasma current (and pedestal pressure, proportional to I_{p2}) and, without mitigation at 3.8MA, in JET, ELMs may reach ~0.8MJ. These large ELMs deposit high power density on the divertor plates, and may cause material ablation, especially from C co-deposited layers. One hypothesis to explain the non-stationary character of the high Ip H-modes is therefore related to the influx of impurities caused by the increasing ELM size. This is consistent with the observation [12] that above a certain threshold of ΔW_{ELM} (~0.6MJ) (inner divertor) the large ELM causes strong impurity influxes in the divertor, with radiation spilling over to the outboard X-point region leading to significant radiation inside the separatrix. The associated strong divertor cooling drives the inner divertor into detachment after the ELM crash resulting in a (transient) type III phase, with reduced confinement. The enhanced radiation losses result from the ablation of co-deposited carbon layers. These results are in line with the analysis reported in this paper where for I_p>3.5MA (ΔW_{ELM}~0.6MJ see figure 10(a)) ELM control by gas fuelling was required to reduce the ELM size and maintain stationary conditions.

Several experiments have indicated a correlation between ELM size and pedestal parameters before an ELM with collisionality being the best ordering parameter [13]. The results for this experiment agree with this dependence as shown in figure 10(b), although (as for the rest of the database) we observe a relatively large spread of ELM size for a given collisionality in the collisionality range explored in these experiments. Figure 11 shows the dependence of the normalised ELM energy loss (ΔWELM/Wped) on local pedestal ρ^*. Although the figure could suggest a possible dependence with ρ^*, this dependence may be artificial. In these experiments we are changing the absolute ELM size and the pedestal ρ^* by both changing I_p and B_T as normal, but also by strong gas puffing the edge to control the ELM size. The gas required to moderate the ELMs at low ρ^* reduces confinement and β_N and increases ρ^* by reducing the pedestal temperature.

6. PEDESTAL CHARACTERISTICS AND STRUCTURE

The prediction and understanding of the Edge Transport Barrier (ETB) and how it can be extrapolated to ITER, is crucial for the determination of ITER performance. The contribution from the pedestal to the overall plasma stored energy, the strength of the barrier and in particular, the temperature at the top of the barrier affects the ion temperature profiles in the core. Figure 12(a) shows the ne–Te (T_i~1.2-1.5T_e) diagram for the different values of plasma

current with the pedestal values averaged over a period of ~20ms before a type I ELM. The temperature is calculated averaging the measured profiles from HRTS and ECE and the density from HRTS. Also shown are the lines (full) of constant pedestal plasma pressure and the expected pedestal density and temperature (dotted) extrapolated from a 3MA discharge with $H_{98(y,2)} = 1$. It assumes an increase of I_p at constant $n_{e,ped}$ (= 50% of n_{GDL}). It suggests that for the high plasma current pulses, it would still possible to further reduce the pedestal density hence increase the pedestal temperature if no control of the ELM size with gas were required.

The temperature and density pedestal width were analysed for the high plasma current database. Both the pedestal density and temperature width ranges from ~1.5±0.3cm confirming previous JET results [14].

In figure 12(b) the thermal energy (W_{th}) shows a robust correlation with the pedestal stored energy for plasma currents below ~4MA. For higher plasma currents, W_{th} stays approximately constant for increasing W_{ped}. The apparent need to limit ELM size and consequent restriction of pedestal temperature seems to affect the core temperature profiles. A closer analysis of the density and temperature profiles for two different values of Wped at the same I_p (figure 13) shows that, as gas fuelling is added, the edge and core temperature decrease consistent with profile stiffness while for the pedestal density increases and the core density stays approximately constant. The fact that the plasma stored energy does not increase with plasma current as expected can be simply explained by cooling of the edge as a consequence of the gas fuelling required to control the ELMs. With relatively stiff profiles, the core temperatures will not increase even with the increase of the power flux and although gas fuelling was necessary to achieve stationary discharges is a strong candidate as a possible contributor for the observed plasma confinement degradation.

7. SUMMARY AND CONCLUSIONS

Operation at high plasma current up to 4.5MA has been successfully achieved for stationary ELMy H-modes. The results show a plasma performance similar to that achieved in previous experiments at JET. At high current, it was possible to operate at $P_{LOSS}/P_{L-H} \sim 1.7$ with the power available (~27MW). Nevertheless, $H_{98(y,2)} \sim 1$ at $I_p = 4.5$MA could not be achieved.

As plasma current is increased it becomes more challenging to obtain stationary ELMy Hmodes, even at input powers twice above the L-H threshold. This is attributed to plasma-wall interactions, becoming more prominent with increasing absolute ELM size as the plasma current is increased. Above an ELM size of $\Delta W_{ELM} \sim 0.6$MJ ablation of carbon co-deposited layers in the divertor due to ELM impact cause impurity influxes, resulting in strong plasma radiation. Hence, stationary H-modes at high current could be achieved only by controlling the ELM size. The only ELM control method available in JET at this plasma current is strong deuterium gas fuelling.

The pedestal and thermal energy show a robust correlation with $W_{ped} \sim 40\% W_{th}$ up to 3.8MA. Above 3.8MA the increase of the thermal energy is below the prediction from the $IPB_{98(y,2)}$ scaling law. A lower than expected pedestal energy is obtained, most likely due to the cooling of edge

plasma caused by the strong gas fuelling to control the ELM size. In these conditions also the core plasma temperature does not increase proportionally to the plasma current, even with an increase of power flux, likely caused by temperature profile stiffness.

A ρ^* scan where β_N and ν^* were matched show a dependence of normalized confinement with (ρ^*)-2.7, similar to the results obtained in [7]. A comparison of the data set presented here with this scaling shows that for high plasma currents the normalized confinement deviates from the scaling. Constant β_N and ν^* conditions were not obtained above $I_p = 3.5$MA and additional, dedicated experiments at higher plasma current are needed to confirm the scaling at the lowest ρ^* in JET.

The results of the high I_p experiments in JET confirm the role of input power to achieve the required confinement together with the need to control the ELMs to a tolerable size, most likely set by co-deposited layers in the carbon divertor. Although these limitations may not apply to ITER, the JET experiments clearly show that ELM control may also be necessary to maintain stationary plasma performance.

ACKNOWLEDGEMENTS

This work was supported by EURATOM and carried out within the framework of the European Fusion Development Agreement. The views and opinions expressed herein do not necessarily reflect those of the European Commission.

REFERENCES

[1]. Cordey J G et al., Plasma Physics and Controlled Fusion **38** (1996) 1237-1242
[2]. Luce T et al., Plasma Physics and Controlled Fusion **50** (2008) 043001
[3]. ITER physics basis 1998
[4]. Lorne H et al., Nuclear Fusion **39** (1999) 993
[5]. Sartori R et al., Plasma Physics and Controlled Fusion **40** (1998) 757-763
[6]. Cordey J G et al., Proc. 31st EPS Conf. on Plasma Physics (London, UK) vol **28**G (ECA) 1.05 (2004)
[7]. McDonald D et al., IAEA 2004
[8]. Callen J et al., Nuclear Fusion **27** (1987) 1857
[9]. Saibene G et al., Plasma Physics and Controlled Fusion **44** (2002) 1796;
[10]. Martin Y et al., Journal of Physics: Conference Series **123** (2008) 012033
[11]. Chankin A et al., Plasma Physics and Controlled Fusion **41** (1999) 903
[12]. Huber A et al., to be published in Journal of Nuclear Materials (2010)
[13]. Loarte A et al, Plasma Physics and Controlled Fusion **44** (2002) 1815
[14]. Beurskens M et al., Plasma Physics and Controlled Fusion **51** (2009) 124051

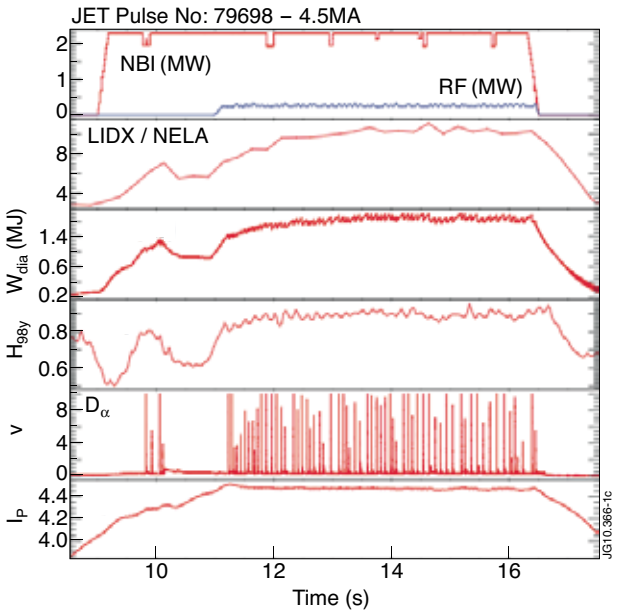

Figure 1: Time traces for a 4.5MA discharge.

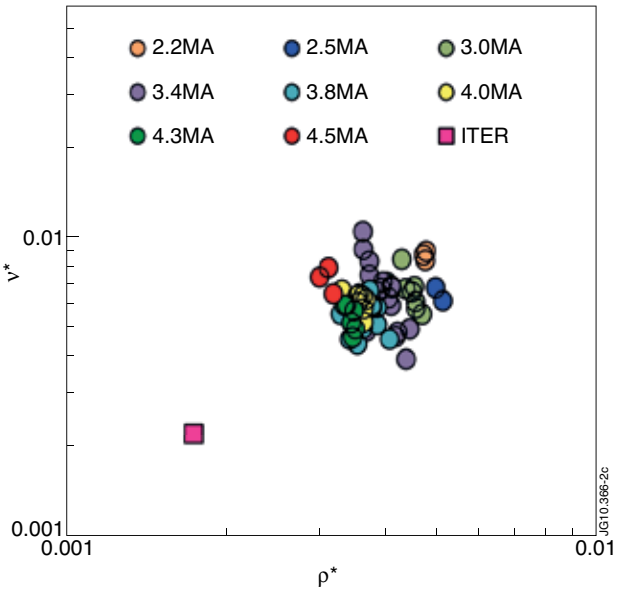

Figure 2: Core ν versus ρ* operational space for the experiments described in this paper. I_p = 2.2MA to 4.5MA. The ITER value for 15MA, Q = 10 is included for comparison.*

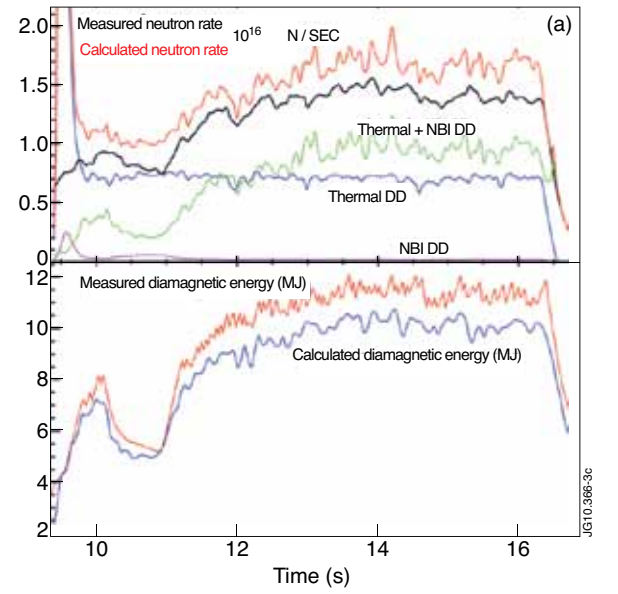

Figure 3: Time traces of the measured and calculated (TRANSP) total neutron rate and diamagnetic energy for Pulse No: 79698. Also shown are the thermal contributions to the total neutron rate.

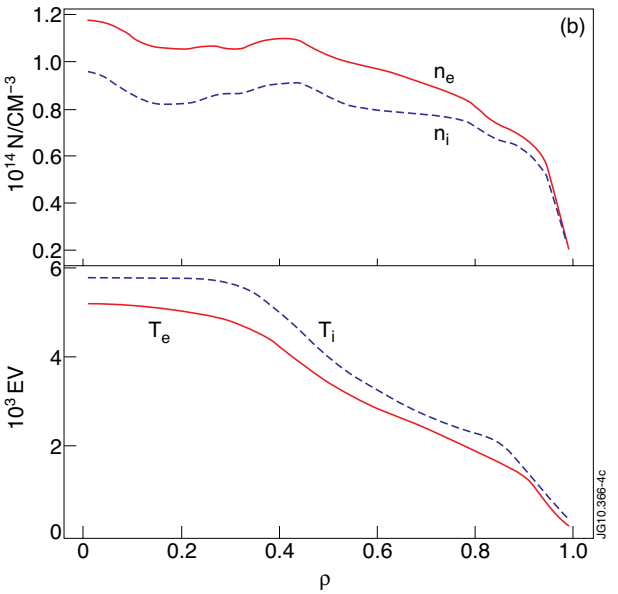

Figure 4: Profiles (TRANSP) of the electron and ion temperature and density for Pulse No: 79698 (Z_{eff}~1.8).

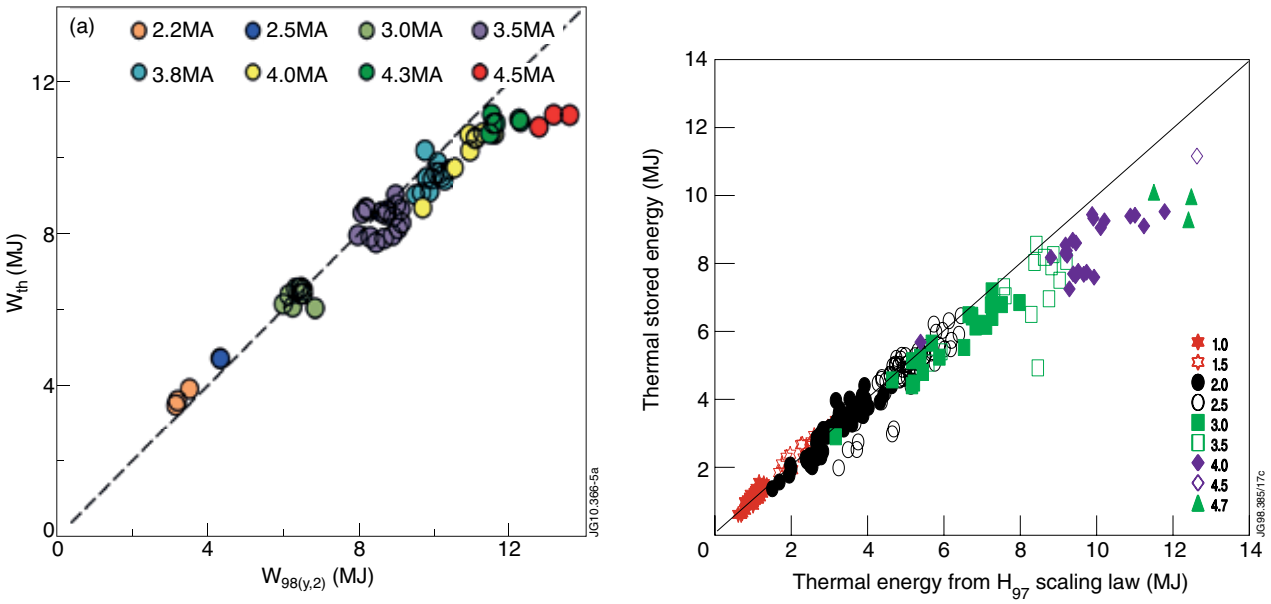

Figure 5: (a) Thermal stored energy versus the thermal energy predicted by the 1998 ELMy H-mode scaling law [4] for recent experiments and (b) thermal stored energy for JET pulses performed in 1996-1999 versus thermal stored energy predicted by the 1997 ELMy H-mode scaling law [1]. Symbols denote plasma current.

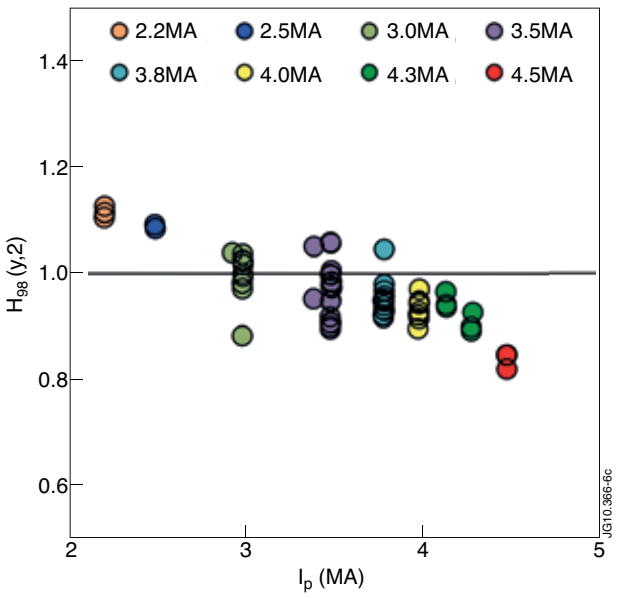

Figure 6: Enhancement confinement factor as function of plasma current.

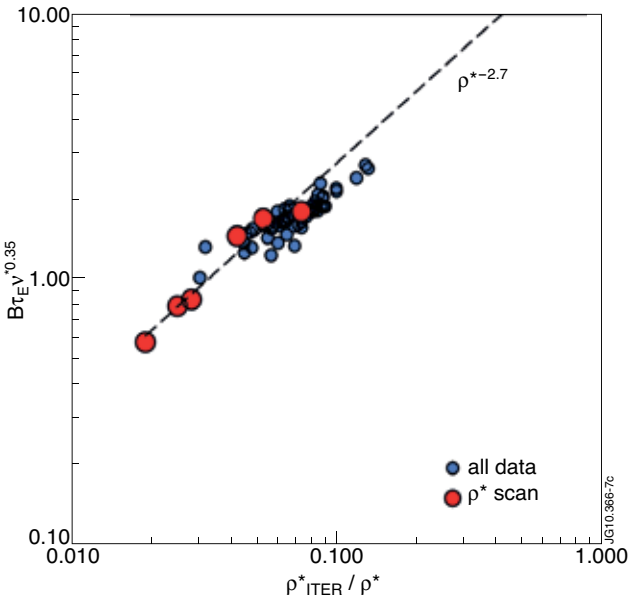

Figure 7: Normalised confinement time ($B\tau_E$) as function of $(\rho^*ITER/\rho^*)^3$.

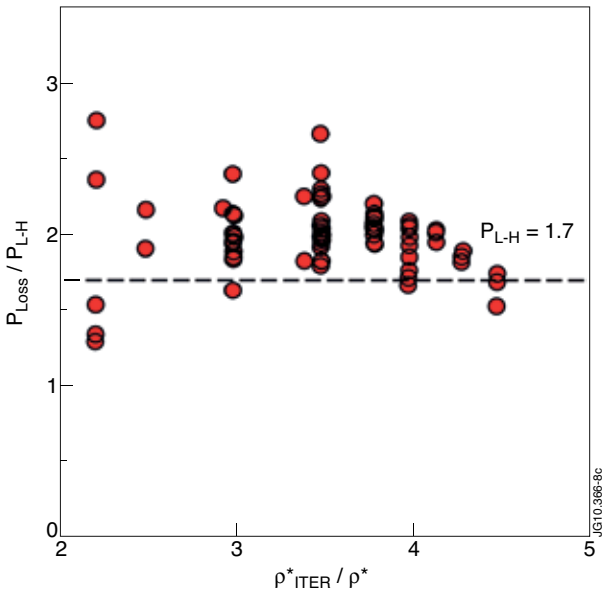

Figure 8: $P_{LOSS}/P_{L\text{-}H}$ as function of I_p.

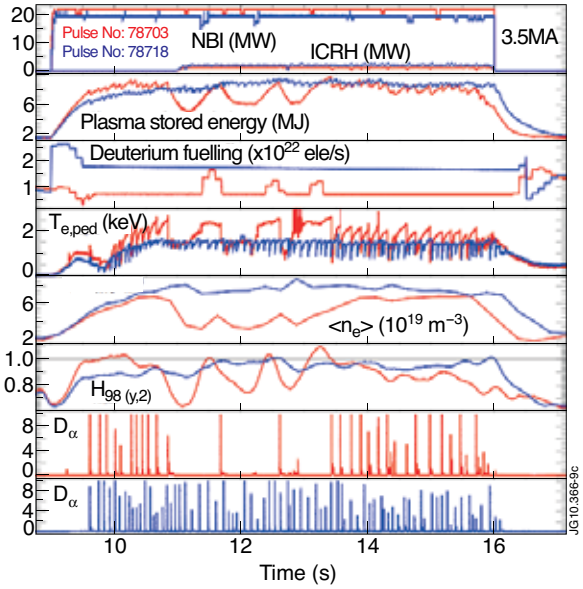

Figure 9: Time traces for two similar pulses, unfuelled (red) and fuelled (blue).

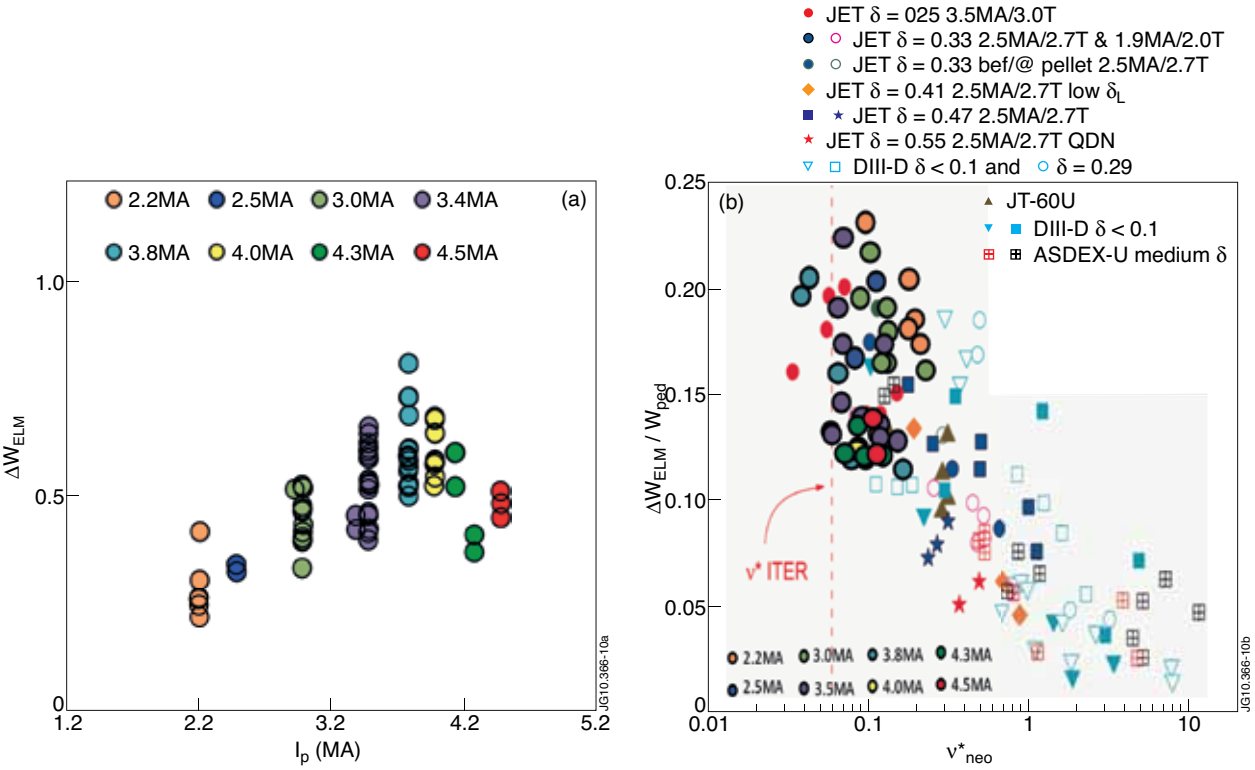

Figure 10: (a) and ELM energy loss as function of plasma current and (b) normalised ELM energy losses ($\Delta W_{ELM}/W_{ped}$) as function of collisionality.

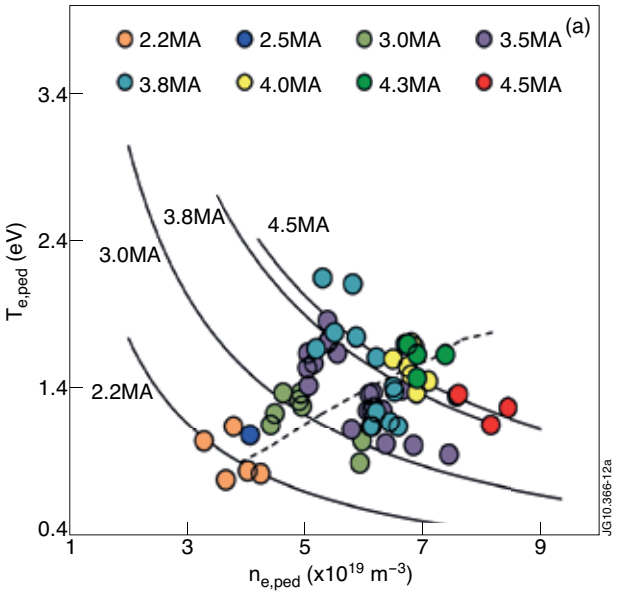

Figure 11: Normalised ELM energy losses as function of local pedestal ρ. Circled points indicate discharges with strong gas fuelling.*

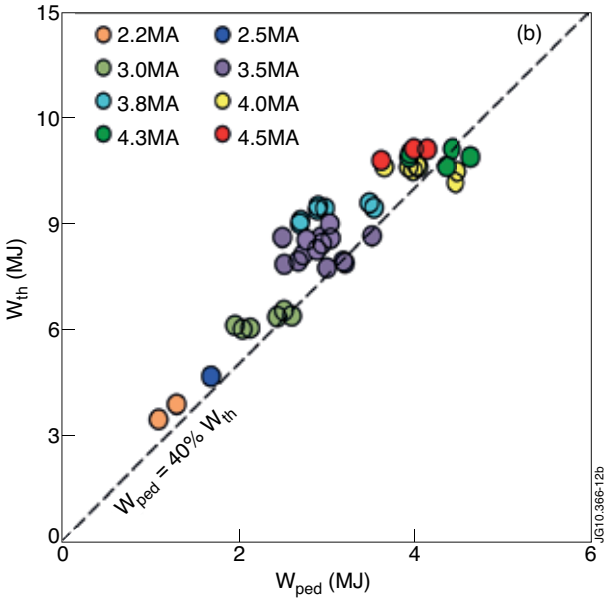

Figure 12: (a) n_e–T_e diagram for increasing plasma current and average natural density assuming $n_{e,ped}$ = 50%n_{GDL} and (b) Thermal energy versus pedestal energy.

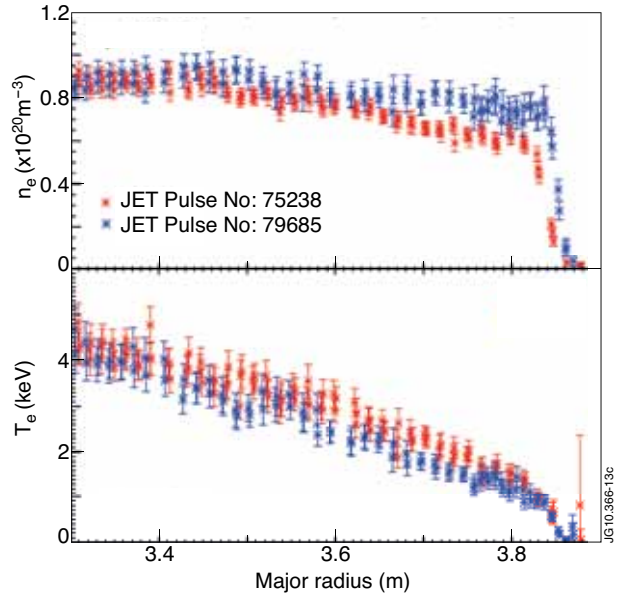

Figure 13: Density and temperature profiles for two pulses with high and low pedestal energy at I_p = 3.5MA.